PHYSIOLOGIA PLANTARUM 107: 201–213. 1999
Printed in Ireland—all rights reserved

ISSN 0031-9317

Pectic epitopes are differentially distributed in the cell walls of potato (*Solanum tuberosum*) tubers

Maxwell S. Bush* and Maureen C. McCann

Department of Cell Biology, John Innes Centre, Norwich Research Park, Colney, Norwich, NR4 7UH, UK
**Corresponding author, e-mail: max.bush@bbsrc.ac.uk*

Received 30 April 1999; revised 22 July 1999

Six monoclonal antibodies (mAbs) were used to map the distribution of pectic epitopes in the cell walls of potato (*Solanum tuberosum* L. cvs Kardal and Karnico) tuber tissue in both light and electron microscopes. Unesterified (mAb JIM 5 epitope) and methyl-esterified (mAb JIM 7 epitope) pectins were abundant and equally distributed in all parenchymal and vascular cell walls. Homogalacturonans (HGAs) involved in Ca^{2+}-cross-linking (mAb 2F4 epitope) were localised to the middle lamella and abundant at cell corners. The tuber cortex was densely labelled, but parenchymal cell walls in the perimedullary region contained few epitopes of calcium pectate except at corners and pit fields. In contrast, pectic side-chains were not detectable in the middle lamella of all parenchymal cell walls, except in the cortex where mAb LM6 (arabinan epitope) labelled the entire wall. The galactan epitope (mAb LM5) was localised to a zone very close to the plasmalemma in cortical cell walls and was also less abundant at pit fields and in vascular cell walls. MAb CCRC-M2 (rhamnogalacturonan I epitope) did not cross-react. Our results show that the cell walls of potato tubers are not homogeneous structures and that the pectic composition of the walls is spatially regulated.

Introduction

Pectin is an ingredient for the food industry, and potato pulp, a waste product remaining after starch extraction (Mayer 1998), is a potentially valuable source of pectins with different commercial functionalities. Despite the commercial importance of potato as a food crop, there have been few studies characterising the cell wall composition of the tuber. In this paper, we use monoclonal antibodies (mAbs) to examine the distribution of pectic molecules in the different tissue types of the tuber.

Three classes of pectin have been described (Carpita and Gibeaut 1993, Voragen et al. 1995). The simplest is homogalacturonan (HGA) which is an unbranched chain of (1→4) linked α-D-GalA residues that can be differentially methyl-esterified and/or acetylated. HGA in its relatively unesterified form is thought to form inter-molecular associations (egg-box junctions and higher order cable structures, Goldberg et al. 1996) with other HGA polymers through Ca^{2+} bridging. Rhamnogalacturonan (RG) I is a branched heteropolymer of alternating (1→2)-α-L-Rha and (1→4)-α-D-GalA residues, interspersed between lengths of HGA homopolymer (Lau et al. 1985). Neutral side-chains composed predominantly of (1→4)-β-D-Gal and/or (1→5)-α-L-Ara residues are anchored to the Rha backbone residues and can bind water through hydrogen bonding. Some RGI side-chains may be cross-linked together via ester bonds between diferulic acid residues (Fry 1983). A high proportion of side-chains raises the water-binding capacity of the molecule, but reduces the gelling ability (reviewed in Hwang and Kokini 1991). RGII (Darvill et al. 1978) has an HGA backbone and the greatest diversity of sugars and linkages of all pectins. Although low in abundance in cell walls, its complex structure is conserved in all species studied to date (Darvill et al. 1978). The formation of borate diester cross-links between apiose residues of RGII has been shown to result in RGII dimer formation in vitro, with consequences for cell wall porosity in vivo (Fleischer et al. 1998). For

Abbreviations – GalA, galacturonic acid; HGA, homogalacturonan; JIM, John Innes monoclonal; LM, Leeds monoclonal; mAbs, monoclonal antibodies; MHR, modified hairy regions; PME, pectin methylesterase; RG, rhamnogalacturonic acid; Rha, rhamnose; TCaS, tris-calcium-saline buffer.

gelation, important parameters are the ratio of branched to unbranched regions of RGI (Hwang and Kokini 1991), the degree of methyl-esterification of HGA and frequency of junction zones and the frequency of RGII dimers along the pectin molecules.

The pectic composition of potato cell walls has been studied previously by Jarvis et al. (1981a) and Ryden and Selvendran (1990) using sequential chemical extractions and shown to be heterogeneous in its extractability. Ca^{2+}-chelators removed 25% of the pectin and these were composed of 77% GalA (a Rha:GalA ratio of 1:40–45) and bore short $(1\rightarrow5)$-linked arabinan and $(1\rightarrow4)$-linked galactan side-chains attached to the rhamnose C-4 of RGI. After Ca^{2+}-chelation, Na_2CO_3 (a de-esterifying agent) extracted a further 27% of the pectin with a 38% GalA content (a Rha:GalA ratio of 1:10–20) and more, longer arabinan/galactan side-chains. A further extraction with KOH removed acidic pectins with a Rha:GalA ratio of 1:5–20 and a large amount of $(1\rightarrow5)$-linked arabinose. A covalently bound, highly branched pectin with unbranched arabinan/galactan side-chains remained in the cellulosic residue. Jarvis et al. (1981b) found that galactanase solubilised 23% of the cell wall carbohydrate. They concluded that the galactan side-chains, which bear 40% of the Ara residues, are the sites of alkali-labile bonds between pectins and perhaps other cell wall components. Schols and Voragen (1994) characterised modified hairy regions (MHR) (degradation products of Rapidase-hydrolysed pectin) from several plants including potato which is highly acetylated (90%) and contains relatively more arabinose.

mAbs are powerful tools to identify and localise pectin in muro and complement the in vitro data from chemical extraction studies. Several anti-pectin antibodies have been generated and some have been used extensively on different tissue types of a range of plant species. mAbs raised to HGA epitopes include mAbs JIM 5, JIM 7 and 2F4, whilst mAb CCRC-M2 labels the RGI backbone and mAbs LM5 and LM6 recognise pectic side-chains. mAbs JIM 5 (Knox et al. 1990) and 2F4 (Liners et al. 1994) both recognise HGA with low degrees of esterification (although the 2F4 epitope is Ca^{2+}-dependent) and generally label the middle lamella, cell corners and the lining of intercellular spaces (reviewed by Knox 1997). In contrast, mAb JIM 7 recognises HGA with at least 35% methyl-esterification and tends to label the entire width of cell walls (Knox et al. 1990). mAb CCRC-M2 recognises sycamore RGI (Puhlmann et al. 1994). Due to their recent introduction (Jones et al. 1997, Willats et al. 1998), the epitope distributions of mAbs LM5 and LM6 (that respectively recognise galactans and arabinans) are less well characterised, although in flax roots (Vicré et al. 1998) and tomatoes (Jones et al. 1997) mAb LM5 labels the wall closest to the plasmalemma.

In order to characterise the potato tuber cell wall, we used this panel of mAbs to map the distribution of pectic epitopes in the parenchymal (starch storage cells) and periderm ('skin') cells of tubers. We developed an immunogold-silver enhancement method for imaging in the confocal laser scanning microscope with resolution of wall domains. Labelling results were confirmed in the electron microscope also using silver enhancement of gold labelling. Our studies show that pectic epitopes are localised to particular wall domains in the potato tuber and that different tissues vary in their pectic composition.

Materials and methods

Tissue preparation for immunocytochemistry

Pieces (2 mm^3) of tissue were sampled from mature *Solanum tuberosum* cv. Kardal and cv. Karnico tubers that had been stored at 4°C for 2 weeks and processed for low temperature L.R. White resin embedding (Wells 1985, Hills et al. 1987). Briefly, the samples were fixed at 20°C for 16 h in 2.5% (v/v) glutaraldehyde (EM grade)-0.05 *M* sodium cacodylate containing 0.05% (v/v) NP-40 (Sigma, Poole, UK). They were then dehydrated for 1 h in each of the following ethanol/water solutions; ice cold 30% and 50% at −20°C, 70% and 90% at −35°C and finally in absolute ethanol at −35°C. The tissue samples were then infiltrated in mixtures (1:1, 1:2 and 1:3) of ethanol/L.R. White resin (Agar Scientific Ltd, Stansted, UK) for 1 h each and then pure resin for 24 h at −20°C. The tissue samples were transferred into individual BEEM capsules (Agar Scientific Ltd) filled with cold resin and polymerised with UV light at −20°C for 24 h and then for 16 h at 20°C.

Immunogold labelling

For light microscopy, 0.5 μm thick resin sections were collected on multiwell glass slides pre-treated with BioBond section adhesive (British BioCell International, Cardiff, UK). Ultrathin sections for electron microscopy were collected on formvar-carbon coated gold grids. Prior to incubation with mAbs JIM 5, JIM 7, LM5, LM6 and CCRC-M2, the sections (both 0.5 μm and ultrathin) were treated with 10% (v/v) sheep serum in phosphate-buffered saline (PBS) to block non-specific labelling. Sections to be incubated with mAb 2F4 were blocked with 5% (w/v) skimmed milk in 20 m*M* Tris-HCl, pH 8.2, 1 m*M* $CaCl_2$, 150 m*M* NaCl (TCaS buffer) according to the method of Liners et al. (1994). The mAbs were applied to sections overnight at 4°C. mAbs JIM 5, JIM 7, LM5, LM6 and CCRC-M2 were diluted 1:50 in 10% (v/v) sheep serum in PBS, whilst 2F4 ascites (1 mg ml^{-1}) was diluted 1:300 in 1% (w/v) skimmed milk in TCaS buffer. The pectic epitopes recognised by these mAbs are: JIM 5, $\leq 50\%$ methyl-esterified HGA (VandenBosch et al. 1989, Knox et al. 1990); JIM 7, $\geq 35\%$ methyl-esterified HGA (Knox et al. 1990); 2F4, a calcium-dependent conformational epitope of at least nine contiguous galacturonic acid residues (Liners et al. 1989, Liners and Van Cutsem 1992); mAb CCRC-M2 recognises the RGI backbone of sycamore pectin (Puhlmann et al. 1994); LM5, $(1\rightarrow4)$-β-D-galactan (Jones et al. 1997); and LM6, $(1\rightarrow5)$-α-L-arabinan (Willats et al. 1998). The sections were then washed with several changes in an excess of the buffer used for diluting the primary mAb and then incubated with gold conjugates (British BioCell International) diluted 1:30 in the respective blocking buffer chosen for the primary mAb. For silver enhancement experiments, a 5 nm gold probe was incubated overnight at 4°C. Sections were washed in buffer as de-

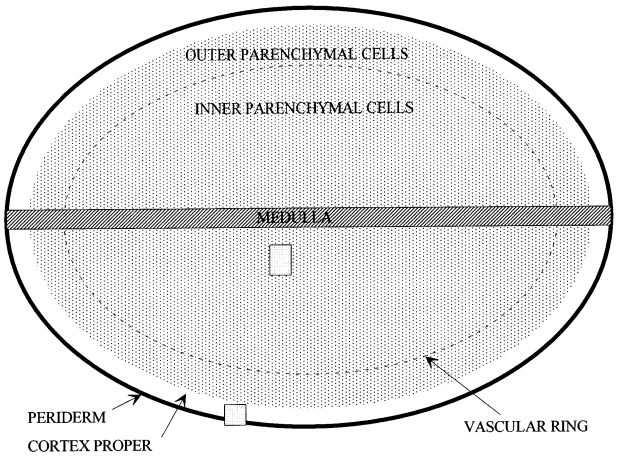

Fig. 1. Simplified diagram of a longitudinal section of a potato tuber showing the different tissue types (perimedullary region is shown stippled) and the areas from which tissue was sampled (small boxes).

scribed above, and antibody complexes cross-linked with 1.0% glutaraldehyde in buffer, and finally rinsed thoroughly with distilled water prior to silver enhancement and counterstaining. Control sections were treated in parallel but with the omission of the primary mAb. Silver enhancement of 5 nm gold probes for electron microscopy was performed for 2 min at 20°C, but this was extended to 10–15 min for light microscopy; the BioCell silver enhancement kit (British BioCell International) was used according to the manufacturer's instructions. Some ultrathin sections were treated for 1 h at 20°C with 100 m*M* sodium carbonate to de-esterify pectins prior to labelling with mAbs CCRC-M2, JIM 5 and JIM 7.

Microscopy

For light microscopy, gold-labelled and silver-enhanced sections were counterstained with basic fuchsin and examined with a Leica TCS NT laser scanning confocal microscope, with excitation and emission wavelengths of 488 and > 515 nm, respectively, using an RT 30/70 mirror. Images of autofluorescence and epi-reflectance were recorded separately, merged using Confocal Assistant 4.02 software and processed with Adobe Photoshop 4.0. A Jeol 1200EX transmission electron microscope was used to examine ultrathin sections counterstained with uranyl acetate and lead citrate.

Results

Distribution of pectic epitopes in different tissues

Thick sections (0.5 μm) of tissue sampled from peripheral and more central regions of the tuber (see Fig. 1) were examined by light microscopy to localise pectic epitopes at the tissue level. The strong reflectance of silver-enhanced gold particles together with the enhanced clarity revealed by merging images of contrasting colours enabled the detection

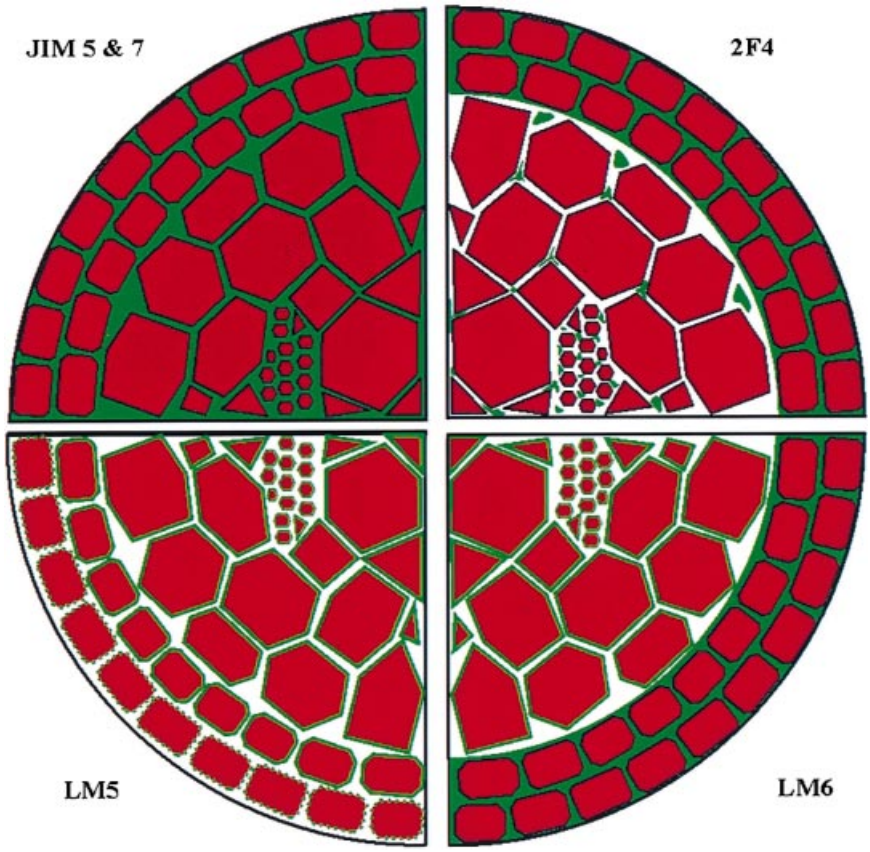

Fig. 2. A summary diagram showing the distribution of pectic epitopes in potato tuber cell walls. Each segment represents a tuber section labelled with mAbs JIM 5, JIM 7, 2F4, LM5 and LM6. The periderm is the outermost black line, the cortex proper is shown as two layers of red cuboidal cells and the storage parenchyma and vascular tissue in the perimedullary region as large and small red polyhedral cells, respectively. The space between the cells is cell wall and gold labelling is shown in green. Both mAbs JIM 5 and JIM 7 label the entire wall throughout the tuber. mAb 2F4 labels the entire wall of the cortical cells, but only the middle lamella at corners in the perimedullary region. Only the primary wall is labelled with mAb LM5 and in the cortex there is a labelling gradient, in cortical walls the middle lamella as well as the primary wall labels with mAb LM6, but not in the perimedullary region.

of weak gold labelling by confocal microscopy. The suberised walls comprising the periderm sectioned poorly, making examination difficult. However, except for mAbs LM6 and 2F4 (see below) it was not appreciably labelled with any of the mAbs used. Secondary walls, such as the thickenings of xylem, did not label with any of the antibodies used. Fig. 2 shows schematically the patterns of gold labelling that were detected in this investigation.

With mAb JIM 5, all cell walls from the cortex proper and perimedullary zone were labelled equally strongly across their entire width and length (Fig. 3A). A similar distribution was seen with mAb JIM 7 except that the labelling was more abundant (Fig. 3B,C). Both mAbs labelled the cell walls of vascular tissue similarly to those of the parenchymal cells (Fig. 3D).

The suberised walls of the periderm were unlabelled with mAb LM5, but all parenchymal cell walls expressed a characteristic pattern of gold labelling that was localised to the primary wall (Fig. 3E). In the cortex proper, only the region of wall closest to the plasmalemma was labelled. Furthermore, the most peripheral layers of cortical cells had walls that labelled lightly and punctately, whilst there was a gradient of epitope abundance over the next few layers of cortical cells until the labelling became continuous. This characteristic labelling of walls with mAb LM5 was modified at pit fields and in the vascular tissue. At pit fields, the labelling appeared to be reduced or abolished, whilst the wall labelling of vascular tissue was greatly reduced in comparison with parenchymal cell walls (Fig. 3F).

The outer walls of the periderm labelled moderately with mAb LM6, but there was no gradient of epitope abundance across the cortex as there was with mAb LM5. mAb LM6 labelled the entire cell wall of cortical cells, but in the perimedullary zone the labelling resembled that observed with mAb LM5 (compare Fig. 3E and G); it was not identical, however, because the mAb LM6 labelling extended more into the middle lamella. The cell walls of vascular cells were labelled less abundantly than parenchymal cell walls (Fig. 3H), but differential labelling at pit fields was not apparent with mAb LM6.

All cell walls were labelled by mAb 2F4. Periderm walls were labelled moderately and those at the boundary of the periderm and cortex proper were labelled more abundantly. Some walls from the latter region were particularly thick and it was in these walls that the distribution of gold labelling was clearly localised to the middle lamella. Throughout the rest of the cortex proper and perimedullary zone, the cell walls were thinner and they appeared to label across their width (Fig. 3I). It was apparent that, deeper into the cortex and in the perimedullary region, cell corners were more densely labelled in comparison with the intervening walls (Fig. 3J and K) and in the latter, only a few corners were labelled and here the labelling was reduced away from the corners (Fig. 3J). The cell walls, especially the corners, of the vascular tissue were more densely labelled than the surrounding parenchymal cell walls (Fig. 3K).

Cell walls did not label with mAb CCRC-M2, even after saponification of sections with 100 m*M* sodium carbonate, when examined at the light or ultrastructural level. All cell walls remained unlabelled when the primary mAbs were omitted in control sections (Fig. 3L).

Ultrastructure of potato tuber cell walls

At the ultrastructural level, small regions of periderm were examined (Fig. 4A). Measurements of cell wall thickness from micrographs are indicated as a range, of which the lower limit represents the wall thickness perpendicular to the plane of the plasma membrane (a range is given because of the difficulty of defining the sectioning angle).

The suberised walls of the periderm varied in thickness from 170 nm to 4 μm, with the thinner walls being most peripheral in position. The thin walls possessed a characteristic central electron-dense band (50–110 nm wide, but in the order of 500 nm at junctions with other walls) which was homogeneous in structure and generally labelled very lightly and punctately with all mAbs (Fig. 4A). The thicker walls lacked this dense band, but were instead composed of two homogeneous lamellae that sandwiched a central fibrillar zone (Fig. 4B). The fibrillar region showed a trend of increasing labelling density in walls closer to the cortex proper. With mAbs JIM 5 and JIM 7 the labelling was present only in patches of these walls (Fig. 4B); with mAb 2F4 it was less localised, but more abundant where the electron-opacity of the wall increased; with mAb LM5 the labelling was very light, whilst with mAb LM6 it was more abundant and more uniform across the width of the wall.

Generally, parenchymal walls were most electron-lucent nearest to the plasmalemma, with the middle lamella staining darker (especially so at pit fields). Some walls, however, appeared more homogeneous in density (Fig. 4C–F). At filled cell corners, the middle lamella expanded (Fig. 4F), but in those corners with an intercellular space it was usually reduced to a thin layer around the space (Fig. 4D). Corners where thick walls joined had conspicuous parallel lamellae of alternating electron density and at high magnification fibrils radiated from the dense lamellae into the more lucent layers to give a 'herring-bone' pattern (not shown). At some corners with an intercellular space, the middle lamella exhibited two parallel electron-dense 'tram-lines', 20–40 nm apart, (which diverged as they contacted the intercellular space) that extended up to several microns into the intervening walls (Fig. 4D). Occa-

Fig. 3. Potato tuber sections gold-labelled with mAbs JIM 5 (A), JIM 7 (B–D), LM5 (E–F), LM6 (G–H) and 2F4 (I–K) then silver-enhanced and viewed by confocal microscopy. An image of a control-treated section is shown in panel L. Images A,C,D,F,H,J,K,L are of perimedullary tissue, whilst images B,E,G,I are of cortex proper. Single arrows indicate filled corners, double arrows indicate corners with intercellular spaces, arrowheads show pit fields, brackets show vascular tissue and asterisks show spaces once occupied by starch granules. All scale bars are 20 μm.

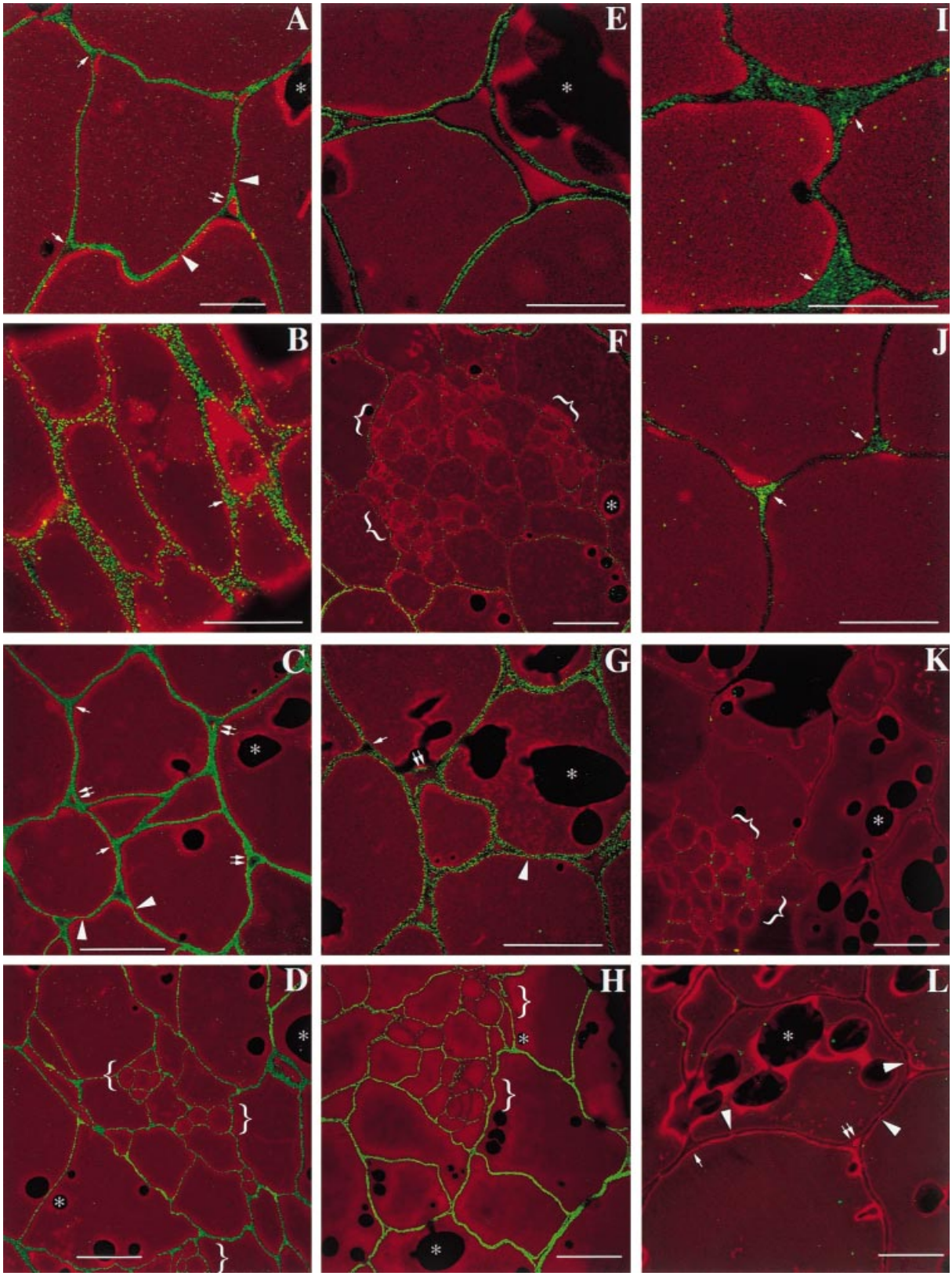

Fig. 3.

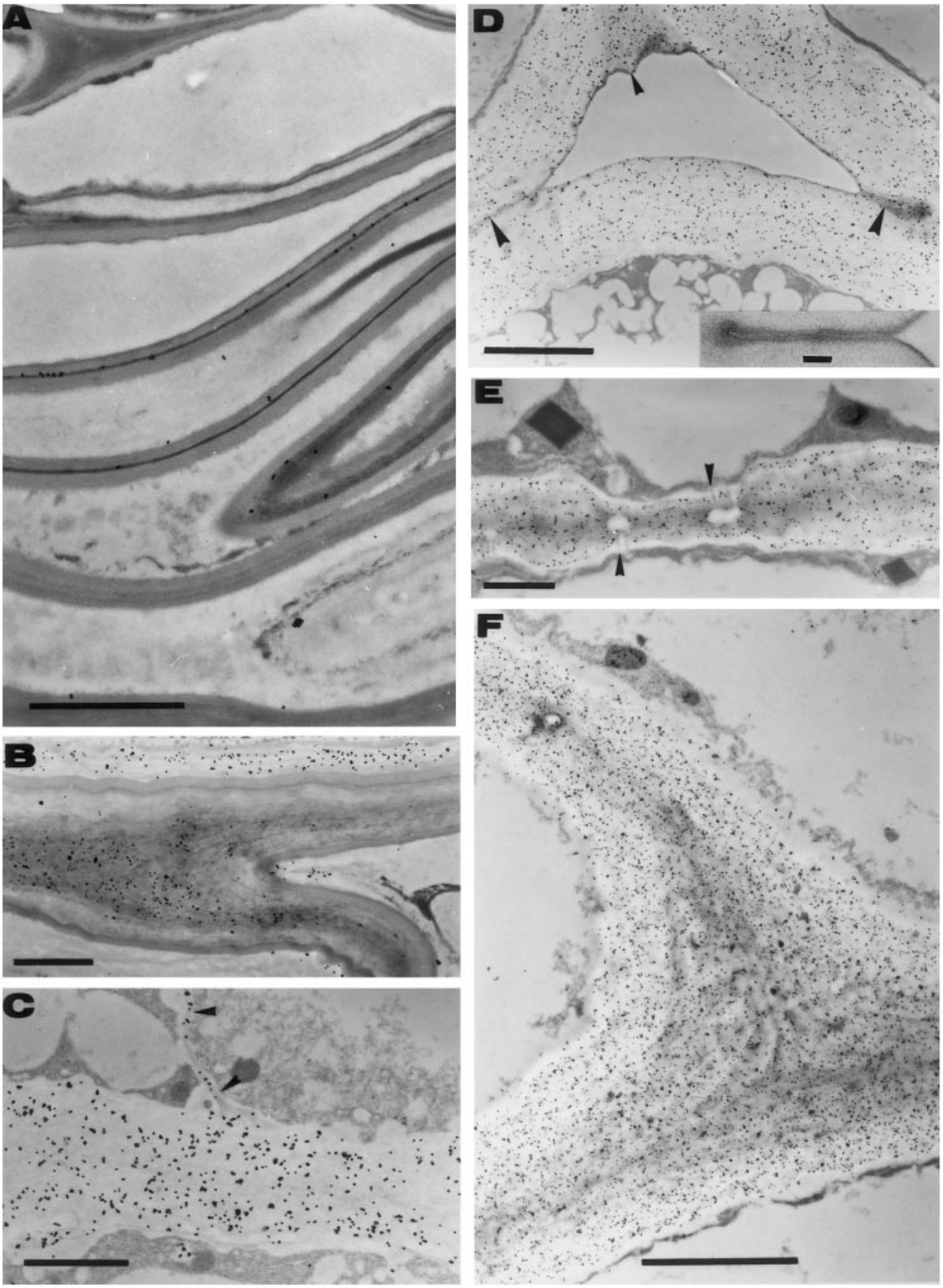

Fig. 4.

sionally, corners with intercellular spaces were observed with a highly fibrous middle lamella matrix that was fraying.

All parenchymal cell walls (1–2 μm thick) were labelled across their width and entire length by both mAbs JIM 5 and JIM 7 (Fig. 4C–F), including thin (70 nm) newly formed walls (Fig. 4C). Both mAbs JIM 5 and JIM 7 labelled the walls of vascular cells like those of the parenchymal cell walls. Sections treated with 100 m*M* sodium carbonate to de-esterify pectins showed an increased labelling density with mAb JIM 5, but in contrast, labelling with mAb JIM 7 was dramatically reduced.

The characteristic pattern of mAb LM5 labelling seen by confocal microscopy was confirmed at the ultrastructural level (Fig. 5). Throughout the tuber, the gold label was consistently localised to the primary wall (Fig. 5A,B,D), the middle lamella was not labelled at all (Fig. 5C,D). The only variations to this pattern were firstly, the labelling density was lighter in walls from the outer layers of the cortex proper (Fig. 5B) and secondly, the walls of vascular cells (Fig. 5E), new thin parenchymal walls and pit fields showed reduced labelling.

mAb LM6 abundantly labelled the walls of the cortex proper across their width (Fig. 6A), but in the perimedullary zone, the labelling of parenchymal walls was predominantly localised to the primary wall but extended slightly into the middle lamella (Fig. 6B). At cell corners, the expanded middle lamella was labelled very lightly or not at all (Fig. 6C), whilst at corners with intercellular spaces, the wall 'tram-lines' and the electron-dense material surrounding the space were unlabelled (Fig. 6D). Newly formed thin walls were only labelled very lightly (Fig. 6C). There was no differential labelling at pit fields (Fig. 6A) and vascular cell walls showed a reduced intensity of gold labelling compared with the parenchymal cell walls (Fig. 6E).

With mAb 2F4, the labelling pattern of parenchymal cell walls was strikingly different from that seen with the other mAbs: it was localised to the middle lamella (Fig. 7). The electron-dense middle lamella of the thick peripheral cortical walls labelled particularly abundantly. Throughout the rest of the tuber, the parenchymal cell walls were labelled less abundantly (Fig. 7A) and this was particularly apparent in the perimedullary zone, where the walls were labelled very lightly and only a few cell corners were labelled. Generally, the labelling of the middle lamella increased towards cell corners (Fig. 7B) and was most dense on the electron-dense material surrounding intercellular spaces (Fig. 7C) or at filled corners (Fig. 7B). 'Tram-lines' at corners with intercellular spaces were also labelled (Fig. 7C). The density of mAb 2F4 labelling increased at pit fields where the plasmodesmata traversed the middle lamella (Fig. 7A,C). Newly formed thin walls in which a middle lamella was not conspicuous were either labelled extremely lightly or not at all. Thicker parenchymal walls and large corners tended to show a less localised distribution of gold particles, so that even though the middle lamella remained well labelled some gold occurred more peripherally in the primary wall (Fig. 7D). As in other tissues, the walls of the vascular cells were more abundantly labelled at cell corners than in the intervening walls by mAb 2F4 (Fig. 7E).

Discussion

Pectins comprise the most heterogeneous class of cell wall polymers. Our studies show that different pectic epitopes are present in different regions of tuber cell walls. We find that HGA epitopes are uniformly distributed throughout the walls of the different tuber tissues, Ca^{2+}-cross-linked HGA is localised to the middle lamella and side-chains of RGI are generally restricted to the primary wall. The relative distribution of antibody labelling in different tuber tissues and wall domains is summarised in Fig. 2.

The periderm walls appear different to the multi-lamellate ultrastructure described by Dean et al. (1977) and Soliday et al. (1979) and contain few detectable pectic epitopes. The former may be a result of differences in tissue fixation. Our protocol omitted post-fixation with osmium tetroxide because it interferes with immunolabelling, but osmium is a well-known lipid fixative and its use would accentuate the location of the wax layers in the peridermal walls. GLC-MS and NMR data indicate that potato suberin consists of fatty acids, fatty alcohols and other aliphatic, aromatic and phenolic constituents (Kolattukudy and Dean 1974, Garbow et al. 1989) that reduce water loss and pathogen invasion. Garbow and colleagues (Garbow et al. 1989, Stark and Garbow 1992) reported that 50% of the suberised material is cell wall polymer and that suberin binds to cell wall components at discrete sites via aromatic groups. The reduced immunoreactivity of the walls may be a consequence of suberin attachment masking epitopes. However, it is equally feasible that pectin is gradually degraded in the periderm resulting in fewer epitopes. All of the mAbs showed an increase in labelling density from the outer to the inner walls.

We have shown for the first time in potato the immunocytochemical distribution of several pectic epitopes. The mAb JIM 5 and JIM 7 labelling patterns are very similar and suggest that $\leq 50\%$ methyl-esterified (acidic) HGA and $\geq 35\%$ methyl-esterified HGA, respectively, are distributed equally on all parenchymal and vascular cell walls. HGA is secreted from the cell in a highly methyl-esterified form. In vitro studies have shown that mixtures of methyl-esterified and unesterified pectins separate into phases, a process that in vivo may result in some of these polymers segregating to the middle lamella (MacDougall et al. 1997). Some methylated HGA may be modified by pectin methylesterase (PME) (Goldberg et al. 1996) and become incorporated into

Fig. 4. Electron micrographs of tuber sections gold-labelled with mAbs JIM 5 (A–D) and JIM 7 (E–F) and then silver-enhanced. Both mAbs give similar labelling patterns. The thin peripheral peridermal walls (A, cortex proper towards the lower edge) label lightly with both mAbs, whilst the thicker inner walls (B) are labelled more densely in patches. Both mAbs label the entire cell wall of parenchymal cells from the cortex proper (C,D) and perimedullary zone (E,F). Newly formed walls are labelled (arrowheads in C), as are pit fields (E, arrowheads indicate plasmodesmata) and cell corners (D, small arrowheads show the electron-dense lining of an apoplastic space, large arrowheads show 'tram-lines' which are shown at high magnification in the inset; F). Scale bars represent 2 μm (A–C), 3 μm (D,F), 1 μm (E) and 200 nm (D inset).

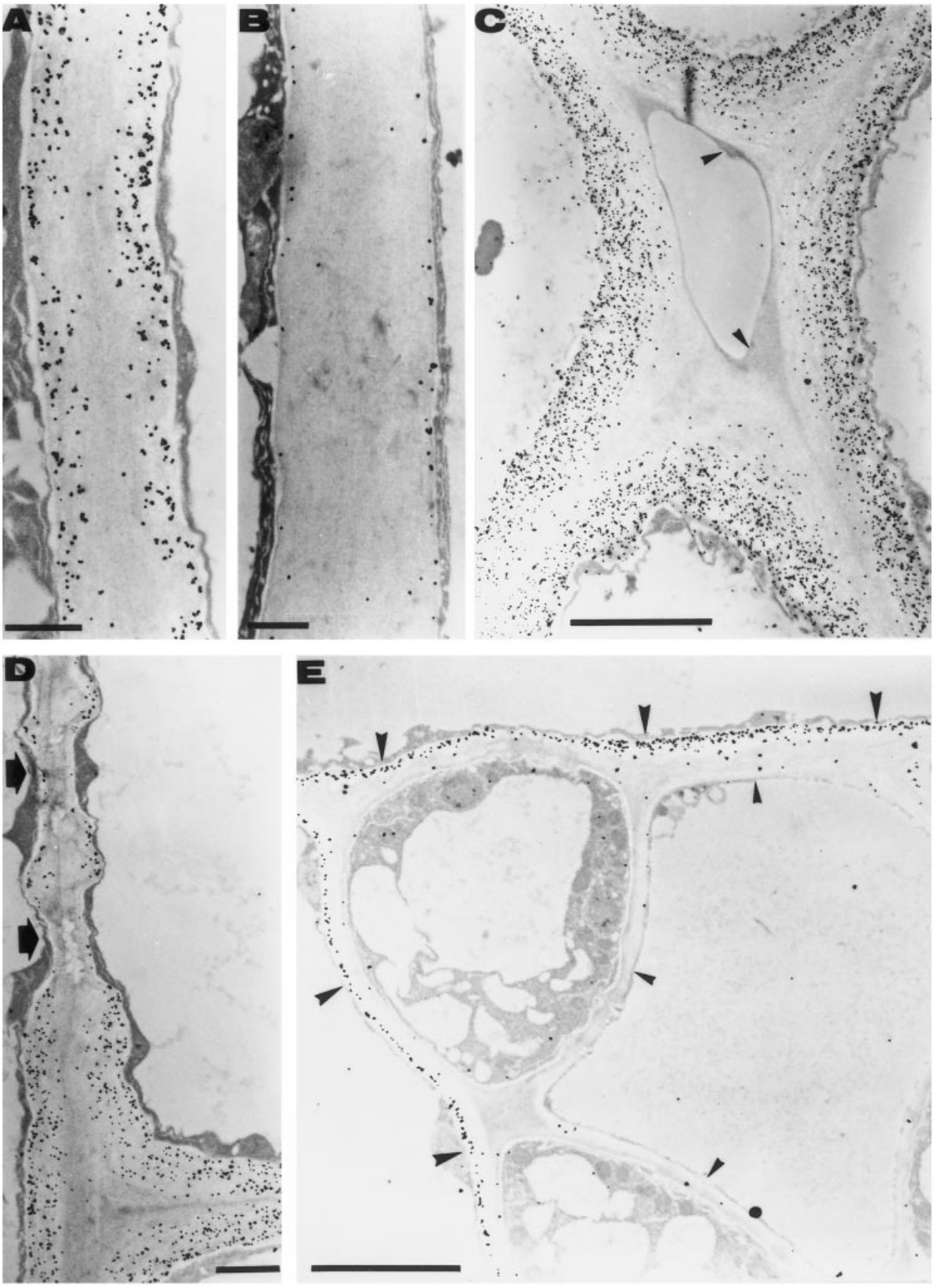

Fig. 5.

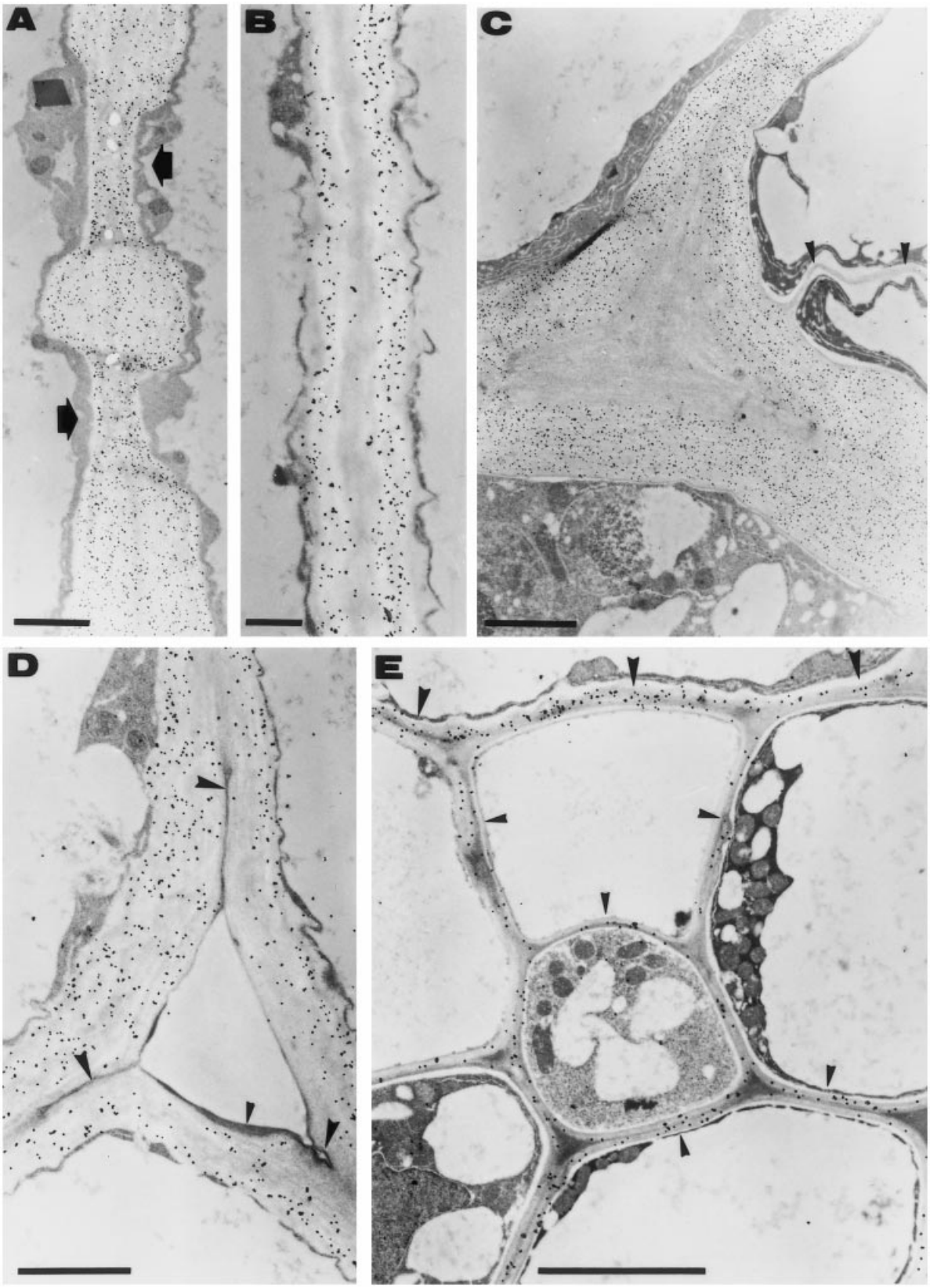

Fig. 6.

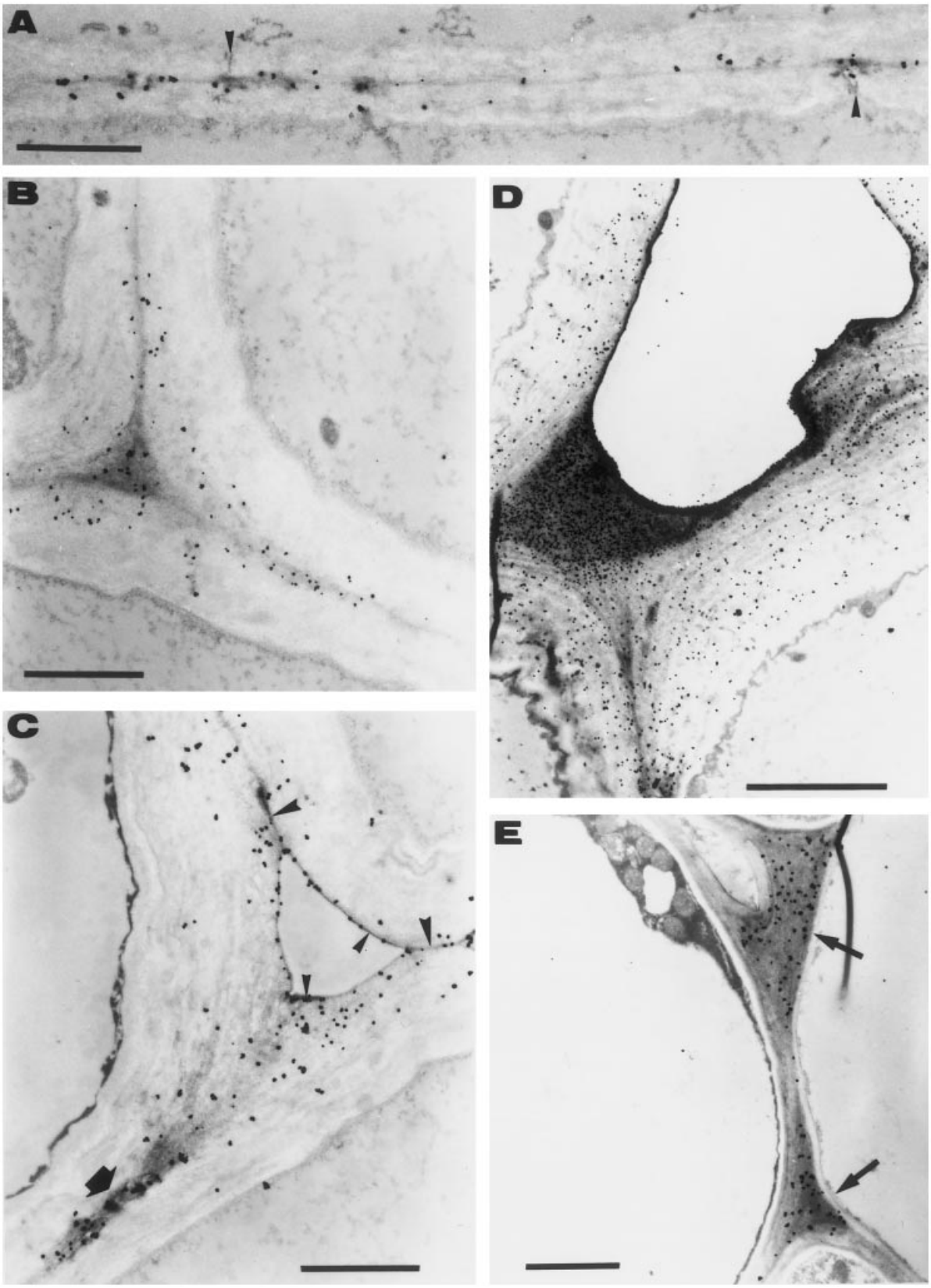

Fig. 7.

the matrix of the cell wall. The low methoxyl mAb JIM 5 and 2F4 epitopes can be generated by PME de-esterification, a process that can occur in a developmental and tissue-specific manner (Knox et al. 1990, Steele et al. 1997). The increased mAb JIM 5 labelling density across the entire wall following sodium carbonate de-esterification, confirmed that the middle lamella is not preferentially enriched in HGA content. The degree of pectin esterification is thought to be a regulating factor in cell-cell adhesion. For instance, in flax cell walls, acidic pectins and PME co-localise to areas of cell-cell contact (middle lamella and cell corners) as well as to plasmadesmata (Morvan et al. 1998), areas in potato that are labelled by mAb 2F4.

Low methoxyl HGAs containing the Ca^{2+}-dependent conformational epitope involved in Ca^{2+}-bridging (mAb 2F4) are essentially localised to the middle lamella in potato tubers, especially where it expands to fill cell corners. This epitope is scarce in new primary walls in which a conspicuous middle lamella has yet to be secreted and in walls from the perimedullary zone. In contrast, it is more abundant in the thick walls subjacent to the periderm, at cell corners and at pit fields. The middle lamella is considered to be the site where adjacent cell walls are cemented together. Cell wall extraction with Ca^{2+}-chelators is traditionally thought to remove middle lamella pectins (Jarvis et al. 1981a, Redgwell and Selvendran 1986, Ryden and Selvendran 1990) and causes disruption to the middle lamella ultrastructure (Jauneau et al. 1998) and cell separation (McCann and Roberts 1991). The middle lamella ultrastructure of potato walls is also disrupted by pectinase treatment (Shomer and Levy 1988) and by cooking (β-eliminative degradation and solubilisation of pectin), the latter resulting in increased cell sloughing through diminished intercellular contact (van Marle et al. 1992, 1997). Stresses in the cell wall are greatest at cell corners and especially concentrated at the points where walls diverge around intercellular spaces (Goldberg et al. 1996). To resist these forces, the wall corners are rich in Ca^{2+} (Jauneau et al. 1998) and reinforced with Ca^{2+}-chelatable, unbranched acidic pectins, such pectins form strong gels through Ca^{2+}-bridges (Goldberg et al. 1996). It is these pectins that mAb 2F4 is recognising in potato. The mAb 2F4 labelling of potato pit fields may be related to increased cell adhesion at these domains, which can be likened to spot welds that protect the delicate plasmodesmata from mechanical damage caused by cell expansion. Tuber enlargement is mainly due to perimedullary parenchymal cells dividing in random orientations and expanding, this causes the separation of vascular tissue as discrete bundles in the perimedullary zone (Xu et al. 1998). The significance of the more abundant mAb 2F4 labelling (stronger cell-cell adhesion) of the vascular cell walls may be to keep vascular cells together as a unit during the growth of the perimedullary zone.

Kollöffel and Linssen (1984) observed structures associated with electron-dense material in parenchymal cell walls of pea cotyledon that resemble the 'tram-lines' reported here and that demarcated the limit of dissolution of material in filled corners to form intercellular spaces. The electron-dense material at the corners of spaces in pea walls was not apparent in potato. However, we speculate that the potato 'tram-lines' are an architectural modification of the middle lamella to allow the stresses concentrated at corners to separate the walls in a controlled manner to form an intercellular space.

The $(1\rightarrow4)$-β-D-galactan epitope recognised by mAb LM5 is localised at the primary cell wall in potato tubers, especially the zone close to the plasmalemma of cortical cells. A similar pattern was described in tomato by Jones et al. (1997) and in flax by Vicré et al. (1998). Primary cell walls contain more highly branched RGI substituted with galactan/arabinogalactan side-chains that are anchored in the wall by alkali-labile (Na_2CO_3-extractable) bonds (Redgwell and Selvendran 1986, Ryden and Selvendran 1990, McCann and Roberts 1991). Potato pectins are rich in galactan (Jarvis et al. 1981a) and galactanase treatment can hydrolyse as much as 23% of the cell wall material (Jarvis et al. 1981b). The similar labelling patterns obtained with mAbs LM5 and LM6 suggest a partial co-localisation of the $(1\rightarrow4)$-β-D-galactan and $(1\rightarrow5)$-α-L-arabinan epitopes. This is not surprising, since Jarvis et al. (1981b) had previously shown that nearly half of the arabinose residues are carried on the galactan side-chains of potato cell walls. However, notable differences in the distribution of these two epitopes occur. In the cortex proper, all walls label strongly with mAb LM6, whilst with mAb LM5 there is a gradient of epitope abundance. mAb LM6 labels middle lamellae of cortical cells except where they expand at cell corners and with a reduced density in perimedullary parenchymal walls,

Fig. 5. Electron micrographs showing the distinctive mAb LM5 labelling pattern of potato tuber cell walls. Gold label is absent from the middle lamella region of all walls (A), and precisely labels a narrow zone of wall close to the plasmalemma in the peripheral cortical layers (B). The expanded middle lamella remains unlabelled at corners with apoplastic spaces (C, arrowheads indicate the electron-dense material lining the space) and filled corners (D). At pit fields (D, arrows) the wall labelling is greatly reduced, as it is on walls of vascular cells (E, large arrowheads show a parenchymal cell wall and small arrowheads indicate the wall of a phloem vessel). Scale bars indicate 1 μm (A,B), 2 μm (D) and 4 μm (C,E).

Fig. 6. Sections of potato tuber tissue immuno-gold labelled with mAb LM6 and then silver-enhanced. In the cortex proper, parenchymal cell walls label in their entirety (A) including pit fields (A, arrowheads), however, in the perimedullary zone the middle lamella labels only sparsely (B). Throughout the tuber, there is no labelling of the expanded middle lamella at cell corners (C–E) or of newly formed walls in the cortex proper (C, arrowheads). The wall 'tram-lines' at corners with intercellular spaces (D, large arrowheads) and the electron-dense material lining the space (D, small arrowheads) do not label with mAb LM6 and walls of vascular cells (E, small arrowheads) label more lightly than parenchymal walls (E, large arrowheads). Scale bars represent 1 μm (B), 2 μm (A,C,D) and 4 μm (E).

Fig. 7. Electron micrographs of potato tuber sections immuno-gold labelled with mAb 2F4 and silver-enhanced. In perimedullary parenchymal cells, the sparse wall labelling is restricted to the middle lamella (A), the labelling density increases at pit fields (A, arrowheads indicate plasmodesmata; C, arrow) and towards corners (B,C). The electron-dense material lining apoplastic spaces at some corners labels abundantly (C, small arrowheads; D) as do wall 'tram-lines' (C, large arrowheads). The label is more widely distributed at large corners (D). The labelling of vascular cell walls, like that of parenchymal walls is generally localised to the expanded middle lamella of corners (E). Scale bars represent 1 μm (B,C,E) and 2 μm (A,D).

but mAb LM5 does not label the middle lamella at all. The LM5 epitope is absent at pit fields and scarce in vascular cell walls both of which label more abundantly with mAb LM6.

Neutral side-chains attached to the RG backbone produce the so-called 'hairy' or branched regions of the polymer. Schols and Voragen (1994) reported that potato MHR (degradation products of Rapidase-hydrolysed pectin) account for 0.04% of the wet tuber weight and are highly acetylated (90%), rich in galactose and comparatively weakly methyl-esterified (13%). MHR from a variety of plants are only hydrolysed by rhamnogalacturonase (following saponification), which yields a characteristic spectrum of oligo- and polymeric degradation products, including a methyl-esterified xylogalacturonan, short segments of highly branched RG backbone and tetra- and hexameric RG oligomers (reviewed by Schols and Voragen 1996).

The side-chains of pectin are flexible (Foster et al. 1996, Ha et al. 1996) and their presence may limit pectin intermolecular associations through entanglements, so reducing gelling (Hwang and Kokini 1991); this correlates with a loss of galactosyl residues from tomato locular tissue upon gel formation (Cheng and Huber 1996). Although we do not know the localisation of the RGI backbone because of the lack of mAb CCRC-M2 cross-reactivity, the differential localisation of the two types of side-chain may have subtly different functions. For example, galactan/arabinan side-chains with t-Ara residues may form diferulate bridges allowing side-chains on pectin molecules to be cross-linked. Side-chains with and without t-Ara residues could regulate wall porosity, whilst the cross-linked side-chains may also contribute architecturally to wall rigidity.

Pectins are the most structurally complex and variable molecules within the cell wall. This diversity may reflect functional differences in cell wall architecture that are important during tuber growth and development.

Acknowledgements – The authors would like to thank Drs J. P. Knox, M. Hahn and P. Van Cutsem for their kind gifts of mAbs and Dr R. Visser for the potato tubers. They are grateful to Sue Bunnewell for photographic assistance, Grant Calder for assistance with the Leica confocal microscope and computer graphics, Nicola Stacey and Mazz Marry for general help and advice and to Brian Wells for readily sharing his considerable experience in electron microscopy. This research was funded by EC network grant CT97 2224 to M. S. B. and a Royal Society University Research Fellowship to M. C. M.

References

Carpita NC, Gibeaut DM (1993) Structural models of primary cell walls in flowering plants: Consistency of molecular structure with the physical properties of the walls during growth. Plant J 3: 1–30

Cheng GW, Huber DJ (1996) Alterations in structural polysaccharides during liquefaction of tomato locule tissue. Plant Physiol 111: 447–457

Darvill AG, McNeil M, Albersheim P (1978) Structure of plant cell walls. VIII. A new pectic polysaccharide. Plant Physiol 62: 418–422

Dean BB, Kolattukudy PE, Davis RW (1977) Chemical composition and ultrastructure of suberin from hollow heart tissue of potato tubers (*Solanum tuberosum*). Plant Physiol 59: 1008–1010

Fleischer A, Titel C, Ehwald R (1998) The boron requirement and cell wall properties of growing and stationary suspension-cultured *Chenopodium album* L. cells. Plant Physiol 117: 1401–1410

Foster TJ, Ablett S, McCann MC, Gidley MJ (1996) Mobility-resolved ^{13}C-NMR spectroscopy of primary plant cell walls. Biopolymers 39: 51–66

Fry SC (1983) Feruloylated pectins from the primary cell wall: Their structure and possible functions. Planta 157: 111–123

Garbow JR, Ferrantello LM, Stark RE (1989) ^{13}C Nuclear magnetic resonance study of suberized potato cell wall. Plant Physiol 90: 783–787

Goldberg R, Morvan C, Jauneau A, Jarvis MC (1996) Methyl-esterification, de-esterification and gelation of pectins in the primary cell wall. In: Visser J, Voragen AGJ (eds) Pectins and Pectinases. Elsevier Science, Amsterdam, pp 151–171

Ha M-A, Evans BW, Jarvis MC, Apperley DC, Kenwright AM (1996) CP-MAS NMR of highly mobile hydrated biopolymers: Polysaccharides of *Allium* cell walls. Carbohydr Res 288: 15–23

Hills GJH, Plaskitt KA, Young ND, Dunigan DD, Watts JW, Wilson TMA, Zaitlin M (1987) Immunogold localisation of the intracellular sites of structural and non structural tobacco mosaic virus proteins. Virology 61: 488–496

Hwang J, Kokini JL (1991) Structure and rheological function of side branches of carbohydrate polymers. J Text Stud 22: 123–167

Jarvis MC, Hall MA, Threlfall DR, Friend J (1981a) The polysaccharide structure of potato cell walls: Chemical fractionation. Planta 152: 93–100

Jarvis MC, Threlfall DR, Friend J (1981b) Potato cell wall polysaccharides: Degradation with enzymes from *Phytophthora infestans*. J Exp Bot 32: 1309–1319

Jauneau A, Roy S, Reis D, Vian B (1998) Probes and microscopical methods for the localisation of pectins in plant cells. Int J Plant Sci 159: 1–13

Jones L, Seymour GB, Knox JP (1997) Localization of pectic galactan in tomato cell walls using a monoclonal antibody specific to (1→4)-β-D-galactan. Plant Physiol 113: 1405–1412

Knox JP (1997) The use of antibodies to study the architecture and developmental regulation of plant cell walls. Int Rev Cytol 171: 79–120

Knox JP, Linstead PJ, King J, Cooper C, Roberts K (1990) Pectin esterification is spatially regulated both within cell walls and between developing tissues of root apices. Planta 181: 512–521

Kolattukudy PE, Dean BB (1974) Structure, gas chromatographic measurement, and function of suberin synthesized by potato tuber tissue slices. Plant Physiol 54: 116–121

Kollöffel C, Linssen PWT (1984) The formation of intercellular spaces in the cotyledons of developing and germinating pea seeds. Protoplasma 120: 12–19

Lau JM, McNeil M, Darvill AG, Albersheim P (1985) Structure of the backbone of rhamnogalacturonan I, a pectic polysaccharide in the primary cell walls of plants. Carbohydr Res 137: 111–125

Liners F, Van Cutsem P (1992) Distribution of pectic polysaccharides throughout walls of suspension-cultured carrot cells. An immunochemical study. Protoplasma 170: 10–21

Liners F, Letesson J-J, Didembourg C, Van Cutsem P (1989) Monoclonal antibodies against pectin. Recognition of a conformation induced by calcium. Plant Physiol 91: 1419–1424

Liners F, Gaspar T, Van Cutsem P (1994) Acetyl- and methyl-esterification of pectins of friable and compact sugar-beet calli: Consequences for intercellular adhesion. Planta 192: 545–556

MacDougall AJ, Rigby NM, Ring SG (1997) Phase separation of plant cell wall polysaccharides and its implications for cell wall assembly. Plant Physiol 114: 353–362

Mayer F (1998) Potato pulp: Properties, physical modification and applications. Polymer Degrad Stab 59: 231–235

McCann MC, Roberts R (1991) Architecture of the primary cell wall. In: Lloyd CW (ed) The Cytoskeletal Basis of Plant Growth and Form. Academic Press, London, pp 109–129

Morvan O, Quentin M, Jauneau A, Mareck A, Morvan C (1998) Immunogold localisation of pectin methylesterases in the cortical tissues of flax hypocotyl. Protoplasma 202: 175–184

Puhlmann J, Bucheli E, Swain MJ, Dunning M, Albersheim P, Darvill AG, Hahn MG (1994) Generation of monoclonal antibodies against plant cell-wall polysaccharides. 1. Characterisation of a monoclonal antibody to a terminal α-(1→2)-linked fucosyl-containing epitope. Plant Physiol 104: 699–710

Redgwell RJ, Selvendran RR (1986) Structural features of cell-wall polysaccharides of onion *Allium cepa*. Carbohydr Res 157: 183–199
Ryden P, Selvendran RR (1990) Structural features of cell-wall polysaccharides of potato (*Solanum tuberosum*). Carbohydr Res 195: 257–272
Schols HA, Voragen AGJ (1994) Occurrence of pectic hairy regions in various plant cell wall materials and their degradability by rhamnogalacturonase. Carbohydr Res 256: 83–95
Schols HA, Voragen AGJ (1996) Complex pectins: Structure elucidation using enzymes. In: Visser J, Voragen AGJ (eds) Pectins and Pectinases. Elsevier Science, Amsterdam, pp 3–19
Shomer I, Levy D (1988) Cell wall mediated bulkiness as related to the texture of potato (*Solanum tuberosum* L.) tuber tissue. Potato Res 31: 321–334
Soliday CL, Kolattukudy PE, Davis RW (1979) Chemical and ultrastructural evidence that waxes associated with the suberin polymer constitute the major diffusion barrier to water vapor in potato tuber (*Solanum tuberosum* L.). Planta 146: 607–614
Stark RE, Garbow JR (1992) Nuclear magnetic resonance relaxation studies of plant polyester dynamics. 2. Suberised potato cell wall. Macromolecules 25: 149–154
Steele NM, McCann MC, Roberts K (1997) Pectin modification in cell walls of ripening tomatoes occurs in distinct domains. Plant Physiol 114: 373–381
VandenBosch KA, Bradley DJ, Knox JP, Perotto S, Butcher GW, Brewin N (1989) Common components of the infection thread matrix and the intercellular space identified by immunocytochemical analysis of pea nodules and uninfected roots. EMBO J 8: 335–342
van Marle JT, Stolle-Smits T, Donkers J, van Dijk C, Voragen AGJ, Recourt K (1992) Chemical and microscopical characterisation of potato (*Solanum tuberosum* L.) cell walls during cooking. J Agric Food Chem 45: 50–58
van Marle JT, Clerkx ACM, Boekestein A (1997) Cryo-scanning electron microscopy investigation of the texture of cooked potatoes. Food Struct 11: 209–216
Vicré M, Jauneau A, Knox JP, Driouich A (1998) Immunolocalization of β-(1→4) and β-(1→6)-D-galactan epitopes in the cell wall and Golgi stacks of developing flax root tissues. Protoplasma 203: 26–34
Voragen AGJ, Pilnik W, Thibault J-F, Axelos MAV, Renard CMGC (1995) Pectins. In: Stephen AM (ed) Food Polysaccharides and their Applications. Marcel Dekker, Basel, pp 287–339
Wells B (1985) Low temperature box and tissue handling device for embedding biological tissue for immunostaining in electron microscopy. Micron Microsc Acta 16: 49–53
Willats WGT, Marcus SE, Knox JP (1998) Generation of a monoclonal antibody specific to (1→5)-α-L-arabinan. Carbohydr Res 308: 149–152
Xu X, Vreugdenhil D, van Lammeren AAM (1998) Cell division and cell enlargement during potato tuber formation. J Exp Bot 49: 573–582

Edited by P. Nissen